

Polyakov loop and QCD thermodynamics from the gluon and ghost propagators

Kenji Fukushima

Department of Physics, Keio University, Kanagawa 223-j8522, Japan

Kouji Kashiwa

RIKEN BNL Research Center, Brookhaven National Laboratory, Upton, NY-11973, USA

We investigate quark deconfinement by calculating the effective potential of the Polyakov loop using the non-perturbative propagators in the Landau gauge measured in the finite-temperature lattice simulation. We find that the Polyakov loop shows a first-order and second-order phase transitions for the pure SU(2) and SU(3) Yang-Mills theories, respectively. We also estimate the thermodynamic quantities to confirm quantitative agreement with the lattice data near the critical temperature. We then introduce the effect of dynamical quarks to discuss simultaneous crossovers of deconfinement and chiral restoration. We emphasize that, because the physical contents in the Polyakov-loop effective potential are clear, this method is far advantageous than conventional parameterization to include in-medium screening through the polarization which is missing in most of the QCD phase-diagram research.

PACS numbers: 11.30.Rd, 12.40.-y, 21.65.Qr, 25.75.Nq

It has been a long-standing question in physics of Quantum Chromodynamics (QCD) how to understand confinement of quarks and gluons in the vacuum and how to clarify the nature of deconfinement in a medium in extreme environments (see Ref. [1] for some reviews).

It was Polyakov [2] who first addressed the deconfinement phase transition successfully in the strong-coupling limit of a pure Yang-Mills theory. The order parameter for deconfinement was then identified, which is now called the Polyakov loop. Later on, the strong-coupling expansion was extended to implement quarks and the chiral dynamics [3]. One of the most popular approaches in the QCD phase-diagram research, the chiral effective model (such as the Nambu–Jona-Lasinio model [4–7], the linear-sigma model [8], etc [9]) with the Polyakov loop, is a natural extension along this line.

The largest ambiguity in the P-chiral models lies in the choice of the effective potential of the Polyakov loop. Though the initial choice was motivated by the strong-coupling expansion [4], it is common to use the potential that fits the pure Yang-Mills thermodynamics from the lattice simulation either in a polynomial form [5] or in a Haar-measure form [4, 6]. Since the fitting procedures do not refer to microscopic dynamics at all, it is unclear how the Polyakov-loop potential is related or unrelated to non-perturbative characteristics near T_c as studied in the matrix model [10] (see also Ref. [11] for an insight into the physical contents).

An important breakthrough came from an attempt to understand quark deconfinement in terms of the Landau-gauge propagators that describe gluon confinement [12, 13]. In the Landau gauge it is the deep-infrared enhancement in the ghost propagator that causes confinement, while the gluon propagator is infrared suppressed. This behavior is qualitatively consistent with the confinement scenarios by Kugo and Ojima (they are equivalent

if the ghost renormalization factor diverges at zero momentum [14]) and also by Gribov and Zwanziger [15]. Indeed the gluon and ghost propagators in the Landau gauge at zero and finite temperature have been calculated in the lattice simulation [16–18], the Dyson-Schwinger equation (DSE) [19, 20], the functional renormalization group (FRG) approach [13, 20, 21].

In this Letter we report on an update of Ref. [13] using the state-of-the-art results from the finite-temperature lattice simulation [18] (see Ref. [22] for the finite-temperature propagators in the FRG calculation); only the zero-temperature propagators were used in Ref. [13]. Also, the thermodynamic quantities were not presented in Ref. [13], which will be discussed later.

We would stress, at the same time, that what we address in this Letter is not only an update but should aim to establish a bridge over the common model studies and the first-principle functional approaches. Such a work must be extremely useful for both sides; there are many arguments to suggest that the back-reaction from the matter to the glue sector has crucial impacts on the QCD phase-diagram research based on the P-chiral models [8, 23]. In principle this shortcoming of insufficient back-reaction in the P-chiral models could be resolved with the DSE or FRG approaches [24], but then one has to confront huge-scale computations. As we see later, thanks to a nice parameterization of the propagators in Ref. [18], our calculation strategy in practice requires only minimal modifications in the numerical procedures on the level of model studies. Nevertheless, the outcomes are quite promising as we will see.

In the covariant gauge the gluon propagator inverse can be decomposed into the transverse and the longitudinal parts as

$$D_A^{-1}(p^2) = \left[p^2 Z_A(p^2) T_{\mu\nu} + \xi^{-1} p^2 Z_L(p^2) L_{\mu\nu} \right] \delta^{ab} \quad (1)$$

with $T^{\mu\nu} \equiv g^{\mu\nu} - p^\mu p^\nu / p^2$ and $L^{\mu\nu} \equiv g^{\mu\nu} - T^{\mu\nu}$. Here $Z_A^{-1}(p^2)$ and $Z_L^{-1}(p^2)$ are the transverse and longitudinal dressing functions. In the same way one can introduce the ghost dressing function by $D_C^{-1}(p^2) = p^2 Z_C(p^2)$.

At finite T Lorentz symmetry is broken, so that $T_{\mu\nu}$ should be further decomposed into the temporal or longitudinal $P_{\mu\nu}^L$ and the three-dimensional transverse $P_{\mu\nu}^T$ projections, i.e.

$$P_{\mu\nu}^T \equiv (1 - \delta_{\mu 4})(1 - \delta_{\nu 4}) \left(\delta_{\mu\nu} - \frac{p_\mu p_\nu}{p^2} \right), \quad P_{\mu\nu}^L \equiv T_{\mu\nu} - P_{\mu\nu}^T. \quad (2)$$

Then there appear three distinct gluon propagators; $D_L(p^2)$, $D_T^{(T)}(p^2)$, $D_T^{(L)}(p^2)$ corresponding to the projectors, $L_{\mu\nu}$, $P_{\mu\nu}^T$, $P_{\mu\nu}^L$, respectively.

Interestingly these propagators as well as the ghost propagator are compactly parameterized in a Gribov-Stingl form;

$$D_L = \frac{1}{p^2}, \quad D_T^{(T)} = \frac{c_t d_t (p^2 + d_t^{-1})}{(p^2 + r_t^2)^2}, \quad (3)$$

$$D_T^{(L)} = \frac{c_l d_l (p^2 + d_l^{-1})}{(p^2 + r_l^2)^2}, \quad D_C = \frac{p^2 + d_g^{-1}}{(p^2)^2},$$

as discussed in Refs. [18, 25]. This form also appears in a low-energy effective description of the Yang-Mills theory [26]. We note that we postulated nonrenormalization for the longitudinal gluon propagator because $Z_L = 1 + \mathcal{O}(\xi)$ and $\xi \rightarrow 0$ is taken after all in the Landau gauge. A set of parameters at $T = 0.86T_c$ from Ref. [18] reads;

$$c_t = 5.5 \text{ GeV}^2, \quad d_t = 0.152 \text{ GeV}^{-2}, \quad r_t^2 = 0.847 \text{ GeV}^2, \quad (4)$$

$$c_l = 3.7 \text{ GeV}^2, \quad d_l = 0.221 \text{ GeV}^{-2}, \quad r_l^2 = 0.257 \text{ GeV}^2,$$

that fits the gluon propagators as shown in Fig. 1 and we find that $d_g^{-1} = 0.454 \text{ GeV}^2$ can fit the ghost dressing function as in Fig. 2.

The Gribov-Stingl form is convenient for the practical computation of the partition function and the effective potential of the Polyakov loop. In the present study, we make use of an approximation motivated from the 2-particle-irreducible (2PI) formalism or the FRG equation. In the 2PI formalism for example, the full effective action can be expressed generally as $\Gamma = \frac{1}{2} \text{tr} \ln G^{-1} - \frac{1}{2} \text{tr} \ln (G^{-1} - G_0^{-1}) G + \Gamma_2[G]$ with the full propagator G , the tree-level propagator G_0 , and the sum of the 2PI diagrams $\Gamma_2[G]$. Thus, in the leading-order, the thermodynamic potential is approximated as

$$\beta\Omega_{\text{glue}} \simeq -\frac{1}{2} \text{tr} \ln D_A^{-1} + \text{tr} \ln D_C^{-1}. \quad (5)$$

We note that this leading-order approximation is the theoretical basis for the so-called quasi-particle model of thermodynamics [27]. In other words this truncation works well in the deconfinement regime where gluons are the physical degrees of freedom, while the approximation fails in the confinement regime at low T .

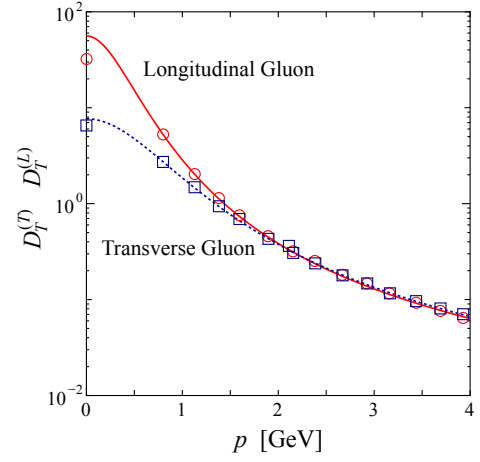


FIG. 1. Three-dimensional transverse and longitudinal propagators $D_T^{(L)}$ and $D_T^{(T)}$ as a function of the momentum. Dots represent the lattice data at $T = 0.86T_c$ from Ref. [18] and the curves represent the fitting results of Eqs. (3) and (4).

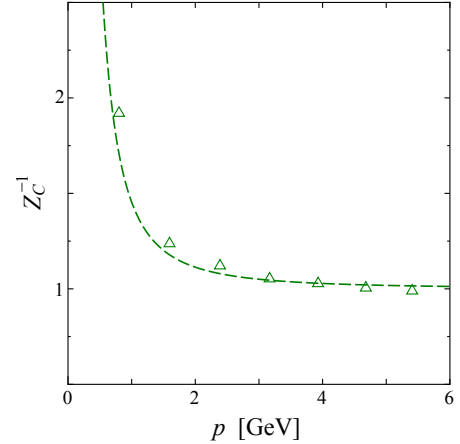


FIG. 2. Ghost dressing function Z_C^{-1} at $T = 0.84T_c$ from Ref. [18] and the curve fitting with $d_g^{-1} = 0.454 \text{ GeV}^2$.

Importantly, one can check the validity of the approximation if necessary, and improve it evaluating the subleading terms and the diagrams contained in Γ_2 once the full propagator is known. We can further simplify Eq. (5) taking the trace over the Lorentz indices to find, $\text{tr} \ln D_A^{-1} = \text{tr} \ln D_L^{-1} + 2\text{tr} \ln D_T^{(T)-1} + \text{tr} \ln D_T^{(L)-1}$.

For the purpose of calculating the effective potential for the Polyakov loop, we keep a background of A_4 in the momentum dependence as the covariant derivative; p^2 in the gluon and ghost propagators should be replaced with $\tilde{p}^2 \equiv (2\pi T n + g\beta A_4)^2 + \mathbf{p}^2$ with A_4 in the adjoint representation. The Polyakov loop is expressed, on the other hand, as $\Phi = (\text{tr} L_3)/3 = (\text{tr} e^{ig\beta A_4})/3$ with A_4 in the fundamental representation.

Then, because the propagators (3) are given as a combination of free forms $(p^2 + m^2)^{-1}$, it is straightforward to carry out the summation over the Matsubara frequency

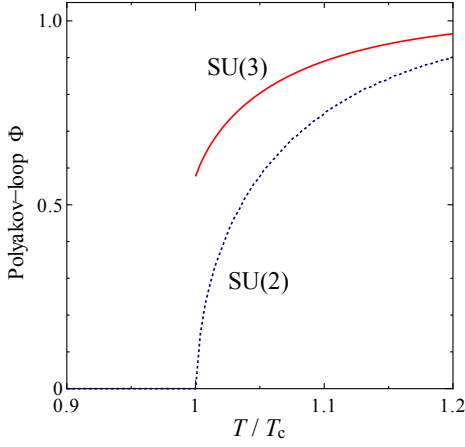


FIG. 3. Polyakov-loop expectation value calculated from the effective-potential minimum for the SU(3) color, as well as the SU(2) case using the same propagators (just for an illustrative purpose).

in an analytical way, i.e. for example,

$$\begin{aligned} \text{tr} \ln D_T^{(T)-1} &= 2\text{tr} \ln(\tilde{p}^2 + r_t^2) - \text{tr} \ln(\tilde{p}^2 + d_t^{-1}) \\ &= 2W_B(r_t^2, L_8) - W_B(d_t^{-1}, L_8), \end{aligned} \quad (6)$$

where we have defined,

$$W_B(m^2, L_8) \equiv -2V \int \frac{d^3p}{(2\pi)^3} \text{tr} \ln(1 - L_8 e^{-\beta\sqrt{p^2+m^2}}) \quad (7)$$

with L_8 being the Polyakov loop matrix in the adjoint representation whose matrix elements are given by $(L_8)_{ab} = 2\text{tr}(t_a L_3 t_b L_3^\dagger)$. We note that we dropped the divergent zero-point energy; it is independent of T and gives an irrelevant offset only. The effective potential $W_B(m^2, L_8)$ can be expressed in terms of Φ and its conjugate $\bar{\Phi}$; the explicit formula is [11],

$$W_B(m^2, \Phi) = -2V \int \frac{d^3p}{(2\pi)^3} \ln\left(1 + \sum_{n=1}^8 C_n e^{-n\beta\sqrt{p^2+m^2}}\right), \quad (8)$$

where $C_8 = 1$, $C_1 = C_7 = 1 - 9\bar{\Phi}\Phi$, $C_2 = C_6 = 1 - 27\bar{\Phi}\Phi + 27(\bar{\Phi}^3 + \Phi^3)$, $C_3 = C_5 = -2 + 27\bar{\Phi}\Phi - 81(\bar{\Phi}\Phi)^2$, $C_4 = 2[-1 + 9\bar{\Phi}\Phi - 27(\bar{\Phi}^3 + \Phi^3) + 81(\bar{\Phi}\Phi)^2]$.

In this way, using Eqs. (5), (6), and (8), we can numerically calculate the Polyakov-loop effective potential and the Polyakov-loop expectation value from the potential minimum as shown in Fig. 3. That is, we first solve $\partial\Omega_{\text{glue}}[\Phi]/\partial\Phi = 0$ to determine $\Phi(T)$ as a function of T , and then calculate thermodynamic quantities using $\Omega_{\text{glue}}[\Phi(T)]$. We find that the critical temperature in our treatment is $T_c = 287$ MeV, which is pretty close to the lattice simulation results in the SU(3) Yang-Mills theory [28]. To check the consistency with the universal argument, we also calculated the Polyakov loop in the

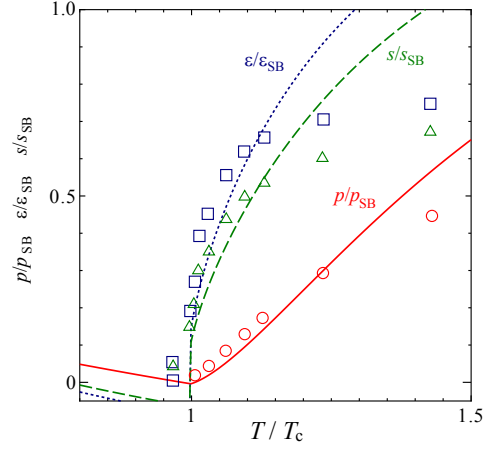


FIG. 4. Thermodynamic quantities normalized by the Stefan-Boltzmann limit for the SU(3) pure Yang-Mills theory. The solid, the dotted, and the dashed lines (the circle, the square, and the triangle symbols) represent the results from our calculation (the lattice simulation [29]) for the pressure, the internal energy density, and the entropy density, respectively.

SU(2) case using the same dressing functions. It should be noted that we show the SU(2) results not for any quantitative intention but only to confirm the right order of the phase transition. We can clearly see the first- and the second-order transitions for the SU(3) and the SU(2) cases, respectively, in Fig. 3. Quantitative agreement with T_c is amazing for its simplicity. The agreement with thermodynamic quantities is, however, less impressive as shown in Fig. 4, though the behavior in the temperature range $T_c \sim 1.2T_c$ looks quite consistent with the lattice data.

The discrepancy above $\sim 1.2T_c$ can be understood from the neglected T -dependence of the propagators that has been seen in Refs. [18, 30]. Once it is correctly taken into account, we expect that the overshoot of thermodynamic quantities could become milder. (We have partially confirmed this.) It should be mentioned that thermodynamic quantities in our calculation naturally approach the Stefan-Boltzmann limit by construction at high temperature. Below T_c we see that the entropy density goes negative in Fig. 4. This is because the negative ghost contribution is too strong, and the approximation to keep only the leading-order contribution in Eq. (5) (which corresponds to a quasi-particle model) breaks down in the confinement regime. Also, in our calculation, we do not include the glueball contribution as is discussed in a recent work [11]. One may think that glueballs are heavy and their effects on thermodynamics are only minor. At finite temperature, however, the electric glueballs can be significantly light and take part in the critical phenomena [31].

Finally we discuss the effects of dynamical quarks and entanglement with the chiral dynamics, which is a phenomenological approach complementary to the field-

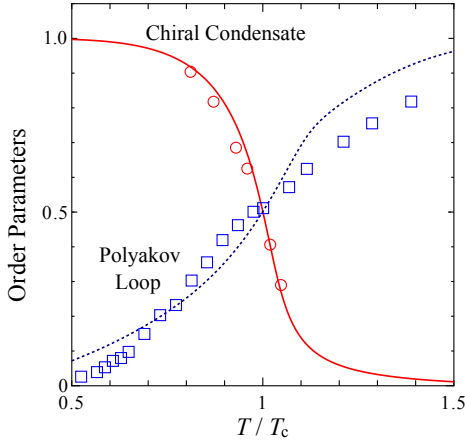


FIG. 5. Polyakov loop and the normalized chiral condensate as functions of T . The dots represent the lattice-QCD results taken from Ref. [34].

theoretical argument [32]. To this end we adopt the covariant coupling in the two-flavor quasi-quark description. Then, the thermodynamic potential from the quark contribution reads,

$$\beta\Omega_{\text{quark}} = -12\beta V \int^{\Lambda} \frac{d^3p}{(2\pi)^3} \sqrt{\mathbf{p}^2 + M^2} - 8W_F(M^2, L_3) + \frac{\beta V(M - m_0)^2}{2G}, \quad (9)$$

where

$$W_F(M^2, L_3) \equiv V \int \frac{d^3p}{(2\pi)^3} \text{tr} \ln \left(1 + L_3 e^{-\beta \sqrt{\mathbf{p}^2 + M^2}} \right), \quad (10)$$

where L_3 is the Polyakov-loop matrix in the fundamental representation. The last term of Eq. (9) represents the condensation energy controlled by a parameter G , which can be interpreted as a mean-field contribution from the interaction in the Nambu–Jona-Lasinio (NJL) model. Thus, we can fix the parameters according to the standard set of the two-flavor NJL model as $\Lambda = 631.5$ MeV, $G\Lambda^2 = 2.2$, and $m_0 = 5.5$ MeV [33]. In this model the chiral condensate is deduced by $\langle \bar{q}q \rangle = (m_0 - M)/(2G)$.

We can express $W_F(M^2, L_3)$ in terms of Φ [5] and solve the Polyakov loop Φ and the chiral condensate $\langle \bar{q}q \rangle$ to minimize the total potential $\Omega_{\text{glue}} + \Omega_{\text{quark}}$. Figure 5 shows our numerical results together with the lattice-QCD data for reference, where we chose $T_c = 178$ MeV (by an arbitrary criterion that Φ takes one half there).

In this case with dynamical quarks thermodynamic quantities behave more reasonably near T_c because quark degrees of freedom dominate over gluons; quark excitations are well under control by Φ . Thermodynamic quantities, the pressure, the internal energy density, and the entropy density, are plotted in Fig. 6. We see that our numerical results quantitatively agree with the lattice-QCD

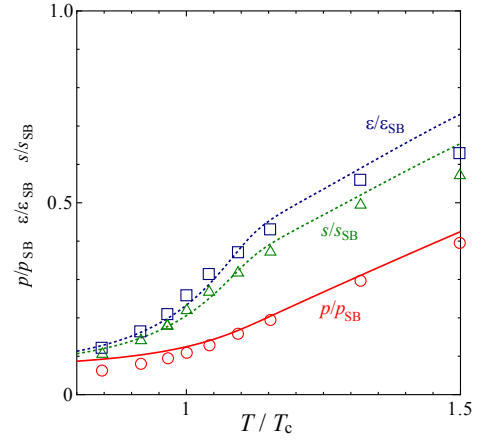


FIG. 6. Thermodynamic quantities normalized by the Stefan-Boltzmann limit with dynamical quarks. The dots represent the lattice-QCD results taken from Ref. [35].

data [35] up to $T \sim 1.4T_c$. We remark here that our calculation is for two flavors and the lattice-QCD simulation for (2+1) flavors, but the difference is minor if normalized by the Stefan-Boltzmann limit, so that the quantitative comparison in Fig. 6 can make physical sense.

Our method with the momentum integration in Eq. (7) is simple enough to be an alternative of the Polyakov-loop potential used in the market of the P-chiral models. Moreover, it is advantageous for our method to be extendable to implement the screening effects through the quark polarization diagrams, which are extremely important to investigate the QCD phase boundaries at high baryon density or strong magnetic field [36]. These effects do not directly couple to gluons, and nevertheless, gluons and thus the nature of deconfinement are affected substantially through the quark loops that carry the baryon number and the electric charge. Progresses in this direction shall be reported elsewhere.

In summary, we elucidated how to construct the effective potential of the Polyakov loop from the non-perturbative propagators of gluons and ghost in the Landau gauge measured in the lattice simulation. This is an extension of the idea of Ref. [13]. We took the fitting forms of the finite-temperature propagators from Ref. [18] and found an easy way to calculate the pressure, the internal energy density, and the entropy density as well as the order parameters as functions of T . We showed that the thermodynamic properties are consistent with the lattice data in the vicinity of T_c . Furthermore we introduced dynamical quarks in the quasi-quark approximation to reproduce the simultaneous crossovers of deconfinement and chiral restoration. We made sure that our potential works well even on the quantitative level without fine-tuning of any parameter. It would be an intriguing future problem to apply our Polyakov-loop potential to the non-local version of the chiral model [37].

Our present work should be a useful step toward the

understanding of the phase structure of QCD matter in extreme environments based on the first-principle-type calculations.

The authors thank Wolfram Weise for kind hospitality at TUM where this work was initiated. They also thank Jens Braun, David Dudal, Michael Ilgenfritz, and Marco Ruggieri for comments. K.F. thanks Jan Pawłowski and Nan Su for useful discussions. K.K. is supported by RIKEN Special Postdoctoral Researchers Program. K.F. is supported by Grant-in-Aid for Young Scientists B (24740169).

-
- [1] K. Fukushima and T. Hatsuda, *Rept. Prog. Phys.* **74**, 014001 (2011), [arXiv:1005.4814 \[hep-ph\]](#); K. Fukushima, *J. Phys. G* **G39**, 013101 (2012), [arXiv:1108.2939 \[hep-ph\]](#).
 - [2] A. M. Polyakov, *Phys. Lett.* **B72**, 477 (1978).
 - [3] E.-M. Ilgenfritz and J. Kripfganz, *Z. Phys.* **C29**, 79 (1985); A. Gocksch and M. Ogilvie, *Phys. Rev.* **D31**, 877 (1985).
 - [4] K. Fukushima, *Phys. Lett.* **B591**, 277 (2004), [arXiv:hep-ph/0310121 \[hep-ph\]](#).
 - [5] C. Ratti, M. Thaler, and W. Weise, *Phys. Rev.* **D73**, 014019 (2006), [arXiv:hep-ph/0506234 \[hep-ph\]](#).
 - [6] S. Roessner, C. Ratti, and W. Weise, *Phys. Rev.* **D75**, 034007 (2007), [arXiv:hep-ph/0609281 \[hep-ph\]](#).
 - [7] W.-j. Fu, Z. Zhang, and Y.-x. Liu, *Phys. Rev.* **D77**, 014006 (2008), [arXiv:0711.0154 \[hep-ph\]](#); M. Ciminale, R. Gatto, N. Ippolito, G. Nardulli, and M. Ruggieri, *Phys. Rev.* **D77**, 054023 (2008), [arXiv:0711.3397 \[hep-ph\]](#); Y. Sakai, K. Kashiwa, H. Kouno, and M. Yahiro, *Phys. Rev.* **D77**, 051901 (2008), [arXiv:0801.0034 \[hep-ph\]](#); K. Fukushima, *Phys. Rev.* **D77**, 114028 (2008), [arXiv:0803.3318 \[hep-ph\]](#).
 - [8] B.-J. Schaefer, J. M. Pawłowski, and J. Wambach, *Phys. Rev.* **D76**, 074023 (2007), [arXiv:0704.3234 \[hep-ph\]](#); B.-J. Schaefer, M. Wagner, and J. Wambach, *Phys. Rev.* **D81**, 074013 (2010), [arXiv:0910.5628 \[hep-ph\]](#); T. K. Herbst, J. M. Pawłowski, and B.-J. Schaefer, *Phys. Lett.* **B696**, 58 (2011), [arXiv:1008.0081 \[hep-ph\]](#); B. Schaefer and M. Wagner, *Phys. Rev.* **D85**, 034027 (2012), [arXiv:1111.6871 \[hep-ph\]](#).
 - [9] E. Megias, E. Ruiz Arriola, and L. Salcedo, *Phys. Rev.* **D74**, 114014 (2006), [arXiv:hep-ph/0607338 \[hep-ph\]](#).
 - [10] A. Dumitru, Y. Guo, Y. Hidaka, C. K. Altes, and R. Pisarski, *Phys. Rev.* **D83**, 034022 (2011), [arXiv:1011.3820 \[hep-ph\]](#); (2012), [arXiv:1205.0137 \[hep-ph\]](#).
 - [11] C. Sasaki and K. Redlich, (2012), [arXiv:1204.4330 \[hep-ph\]](#); M. Ruggieri, P. Alba, P. Castorina, S. Plumari, C. Ratt, and V. Greco, (2012), [arXiv:1204.5995 \[hep-ph\]](#).
 - [12] J. M. Pawłowski, D. Litim, S. Nedelko, and L. von Smekal, *Phys. Rev. Lett.* **93**, 152002 (2004), [arXiv:0312324 \[hep-th\]](#).
 - [13] J. Braun, H. Gies, and J. M. Pawłowski, *Phys. Lett.* **B684**, 262 (2010), [arXiv:0708.2413 \[hep-th\]](#).
 - [14] T. Kugo, (1995), [arXiv:hep-th/9511033 \[hep-th\]](#).
 - [15] D. Zwanziger, *Nucl. Phys.* **B412**, 657 (1994).
 - [16] F. Bonnet, P. Bowman, D. Leinweber, and A. Williams, *Phys. Rev.* **D62**, 051501(R) (2000), [arXiv:hep-lat/0002020 \[hep-lat\]](#); J. Gattnar, K. Langfeld, and H. Reinhardt, *Phys. Rev. Lett.* **93**, 061601 (2004), [arXiv:hep-lat/0403011 \[hep-lat\]](#); A. Cucchieri and T. Mendes, PoS LATTICE , 297 (2007), [arXiv:0710.0412 \[hep-lat\]](#); I. Bogolubsky, E.-M. Ilgenfritz, M. Muller-Preussker, and A. Sternbeck, PoS LATTICE , 290 (2007), [arXiv:0710.1968 \[hep-lat\]](#); T. Iritani, H. Suganuma, and H. Iida, *Phys. Rev.* **D80**, 114505 (2009), [arXiv:0908.1311 \[hep-lat\]](#).
 - [17] A. Cucchieri, T. Mendes, O. Oliveira, and P. Silva, *Phys. Rev.* **D76**, 114507 (2007), [arXiv:hep-lat/0705.3367 \[hep-lat\]](#); A. Sternbeck, L. von Smekal, D. Leinweber, and A. Williams, PoS LATTICE , 340 (2007), [arXiv:0710.1982 \[hep-lat\]](#).
 - [18] R. Aouane, V. Bornyakov, E.-M. Ilgenfritz, V. Mitrushkin, M. Muller-Preussker, and A. Sternbeck, *Phys. Rev.* **D85**, 034501 (2012), [arXiv:1108.1735 \[hep-lat\]](#).
 - [19] L. von Smekal, A. Hauck, and R. Alkofer, *Phys. Rev. Lett.* **79**, 3591 (1997), [arXiv:hep-ph/9705242 \[hep-ph\]](#); *Annals Phys.* **267**, 1 (1998), [arXiv:hep-ph/9707327 \[hep-ph\]](#); R. Alkofer and L. v. Smekal, *Phys. Rept.* **353**, 281 (2001), [arXiv:hep-ph/0007355 \[hep-ph\]](#); C. Fischer, R. Alkofer, and H. Reinhardt, *Phys. Rev.* **D65**, 094008 (2002), [arXiv:hep-ph/0202195 \[hep-ph\]](#); C. Fischer and R. Alkofer, *Phys. Lett.* **B536**, 177 (2002), [arXiv:hep-ph/0202202 \[hep-ph\]](#); C. Fischer and J. M. Pawłowski, *Phys. Rev.* **D75**, 025012 (2007), [arXiv:hep-ph/0609009 \[hep-ph\]](#); D. Dudal, S. Sorella, N. Vandersickel, and H. Verschelde, *Phys. Rev.* **D77**, 071501 (2009), [arXiv:0711.4496 \[hep-th\]](#); A. Aguilar, D. Binosi, and J. Papavassiliou, *Phys. Rev.* **D78**, 025010 (2008), [arXiv:0802.1870 \[hep-ph\]](#); P. Boucaud, J. Leroy, A. Le Yaouanc, J. Micheli, O. Pene, and J. Rodriguez-Quintero, *JHEP* **0806**, 099 (2008), [arXiv:0803.2161 \[hep-ph\]](#); D. Dudal, J. A. Gracey, S. Sorella, N. Vandersickel, and H. Verschelde, *Phys. Rev.* **D78**, 065047 (2008), [arXiv:0806.4348 \[hep-th\]](#); D. Binosi and J. Papavassiliou, *Phys. Rept.* **479**, 1 (2009), [arXiv:0909.2536 \[hep-ph\]](#); P. Boucaud, J. Leroy, J. Micheli, O. Pene, and J. Rodriguez-Quintero, (2011), [arXiv:1109.1936 \[hep-ph\]](#).
 - [20] C. Fischer, A. Maas, and J. M. Pawłowski, *Annals Phys.* **324**, 2408 (2009), [arXiv:0810.1987 \[hep-ph\]](#).
 - [21] F. Marhauser and J. M. Pawłowski, (2008), [arXiv:0812.1144 \[hep-ph\]](#); J. Braun, L. M. Haas, F. Marhauser, and J. M. Pawłowski, *Phys. Rev. Lett.* **106**, 022002 (2011), [arXiv:0908.0008 \[hep-ph\]](#); K.-I. Kondo, *Phys. Rev.* **D82**, 065024 (2010), [arXiv:1005.0314 \[hep-th\]](#).
 - [22] L. Fister and J. M. Pawłowski, (2011), [arXiv:1112.5429 \[hep-ph\]](#); (2011), [arXiv:1112.5440 \[hep-ph\]](#).
 - [23] K. Fukushima, *Phys. Lett.* **B695**, 387 (2011), [arXiv:1006.2596 \[hep-ph\]](#).
 - [24] J. M. Pawłowski, *AIP Conf. Proc.* **1343**, 75 (2004), [arXiv:1012.5075 \[hep-ph\]](#).
 - [25] A. Cucchieri, T. Mendes, and A. Taurines, *Phys. Rev.* **D67**, 091502 (2003), [arXiv:hep-lat/0302022 \[hep-lat\]](#); A. Cucchieri and T. Mendes, PoS FacesQCD , 007 (2010), [arXiv:1105.0176 \[hep-lat\]](#).
 - [26] K.-I. Kondo, *Phys. Rev.* **D84**, 061702 (2011), [arXiv:1103.3829 \[hep-th\]](#).
 - [27] D. Zwanziger, *Phys. Rev. Lett.* **94**, 182301 (2005), [arXiv:hep-ph/0407103 \[hep-ph\]](#).

- [28] G. Boyd, J. Engels, F. Karsch, E. Laermann, C. Legeland, M. Luetgemeier, and B. Petersson, *Nucl. Phys.* **B469**, 419 (1996), [arXiv:hep-lat/9602007 \[hep-lat\]](#); O. Kaczmarek, F. Karsch, P. Petreczky, and F. Zantow, *Phys. Lett* **B543**, 41 (2002), [arXiv:hep-lat/0207002 \[hep-lat\]](#).
- [29] S. Datta and S. Gupta, *Phys. Rev. D* **82**, 114505 (2010), [arXiv:1006.0938 \[hep-lat\]](#).
- [30] C. Fischer, A. Maas, and J. Mueller, *Eur. Phys. J.* **C68**, 165 (2010), [arXiv:1003.1960 \[hep-ph\]](#).
- [31] N. Ishii, H. Suganuma, and H. Matsufuru, *Phys. Rev.* **D66**, 014507 (2002), [arXiv:hep-lat/0109011 \[hep-lat\]](#); Y. Hatta and K. Fukushima, *Phys. Rev.* **D69**, 097502 (2004), [arXiv:hep-ph/0307068 \[hep-ph\]](#).
- [32] J. Braun and A. Janot, *Phys. Rev.* **D84**, 114022 (2011), [arXiv:1102.4841 \[hep-ph\]](#); J. Braun and T. K. Herbst, (2012), [arXiv:1205.0779 \[hep-ph\]](#).
- [33] T. Hatsuda and T. Kunihiro, *Phys. Rept.* **247**, 221 (1994), [arXiv:hep-ph/9401310 \[hep-ph\]](#).
- [34] S. Borsanyi, Z. Fodor, C. Hoelbling, S. Katz, S. Krieg, C. Ratti, and K. Szabo, (2010), [arXiv:1005.3508 \[hep-lat\]](#).
- [35] S. Borsanyi, G. Endrodi, Z. Fodor, A. Jakovac, S. Katz, S. Krieg, C. Ratti, and K. Szabo, *JHEP* **11**, 077 (2010), [arXiv:1007.2580 \[hep-lat\]](#).
- [36] K. Kashiwa, *Phys. Rev.* **D83**, 117901 (2011), [arXiv:1104.5167 \[hep-ph\]](#).
- [37] K. Kashiwa, T. Hell, and W. Weise, *Phys. Rev.* **D84**, 056010 (2011), [arXiv:1106.5025 \[hep-ph\]](#).